KSTLE International Journal, Vol. 2, No. 2, December 2001, pp. 127-132

Operating Characteristics of Counterrotating Floating Ring Journal Bearings

Yeon-Min Cheong† and Kyung-Woong Kim*

Transmission Test Team, Hyundai Motor Company
**Department of Mechanical Engineering, Korea Advanced Institute of Science and Technology*

Abstract : The steady state performance of the counterrotating floating ring journal bearings is analyzed with isothermal finite bearing theory. The effect of counterrotating speed of the sleeve on the performance of the bearing is investigated. It is shown that counterrotating floating ring journal bearings can have considerable load capacity at the same counterrotating speeds, while conventional circular journal bearings with one fluid film cannot. Investigating the relationship between the frictional torques exerted on the ring due to the inner and outer films and the rotational speed of the ring, the stability of the equilibrium state is identified and the operating characteristics of the counterrotating floating ring journal bearing according to the method of acceleration or deceleration of the rotational speeds of the journal and sleeve are clarified. It is theoretically confirmed that floating ring journal bearings can be used in counterrotating journal-bearing system and become good substitutes for rolling bearings in counterrotating systems.

Key words : Counterrotation, floating ring, journal bearing, stability

Introduction

Theoretically, a circular journal bearing with the journal and sleeve counterrotating at the same speeds has no load capacity and cannot serve as a bearing. Therefore, the journal-bearing system with the journal and sleeve counterrotating at almost equal speeds must be supported with different types of bearings rather than the circular bearing.

An example of counterrotating journal-bearing system can be found in the intershaft bearing of the front drive turboshaft engine. Vance [1] writes in his book that "It is sometimes desirable from an aerodynamic design standpoint to have the gas generator shaft and the power turbine shaft rotating in opposite directions, but this may be another problem for the intershaft bearing, especially a fluid-film bearing. A fluid-film bearing with journal and sleeve counterrotating at equal speed has zero load capacity." And he concluded that fluid film bearings cannot be used as counterrotating intershaft bearings.

But, in 1962, Pinkus [2] has already showed by experiment that with the exception of a perfectly circular ungrooved bearing a number of other fluid film bearing designs operate successfully under appreciable load. Geometries of the bearings tested by Pinkus can be classified into two groups, i.e. one is circular or noncircular types of multi-film bearings such as floating ring journal bearings, the other noncircular types such as grooved bearings and tapered land bearing.

A floating ring journal bearing is a special type of journal bearing in which a ring is inserted and kept free to move in the lubricants between the journal and sleeve. With the presence of the two films floating ring journal bearings have been considered that the friction loss is less and stability characteristics better than those of the fixed sleeve bearings. By this reason, floating ring journal bearings are attractive for the high speed turbomachinery applications.

It is interesting fact that a counterrotating floating ring journal bearing with perfectly circular journal, ring and sleeve have considerable amount of load capacity. There are a number of theoretical works on the analysis of the performances of floating ring journal bearings [3-6], but nothing on the counterrotating floatingring ring journal bearings. Hence, the purpose of this paper is to analyze steady state performances of counterrotating floating ring journal bearings and to clarify the operating characteristics of the bearing in order to confirm theoretically that floating ring journal bearings sufficiently support counterrotating journal-bearing system. Isothermal finite bearing theory is used for this work.

Analysis

The geometry of the counterrotating floating ring journal bearing is shown in Fig. 1. As the journal and sleeve rotate at angular velocities ω_j and ω_b about its centers O_j and O_b, respectively, the ring rotates about its center O_r at angular velocity ω_r. Rotational direction of the journal is set to be positive.

To calculate the steady state performances of the bearing, it is necessary to find out the steady state equilibrium positions of the journal and ring centers. The following equations for the force and moment hold for the equilibrium state.

Force Balance

†Corresponding author; Tel: 82-31-369-4860, Fax: 82-31-369-4849
E-mail: ymcheong@hyundai-moter.com

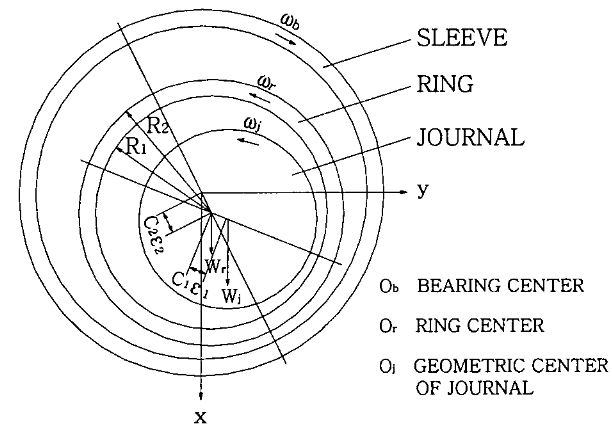

Fig. 1. Counterrotating floating journal bearing.

$$f_{px1} = W_j \quad (1a)$$

$$f_{px2} = W_r + f_{px1} \quad (1b)$$

Moment Balance

$$T_{px1} = T_{j2} \quad (1c)$$

where W_j represents load on the bearing and W_r weight of the ring, f_{px1} and f_{px2} represent the fluid film forces of the inner and outer films, respectively. T_{b1} and T_{j2} represent the torques exerted on the ring by the inner and outer films, respectively.

The performances of the inner and outer films are obtained from the following Reynolds equation for the finite bearings under Reynolds boundary conditions. It is assumed that the surfaces of the journal, ring and sleeve are perfectly circular, and the inner and outer films are always under flooded condition.

$$\frac{\partial}{R\partial\theta}\left(h^3\frac{\partial P}{R\partial\theta}\right)+\frac{\partial}{\partial z}\left(h^3\frac{\partial P}{\partial z}\right) = 6\eta(u_j+u_b)\frac{\partial h}{R\partial\theta} \quad (2)$$

where boundary conditions at each film are

$P=0$ at positions of maximum film thickness

$P=\frac{\partial P}{\partial\theta}=0$ at film rupture boundaries

$P=0$ at axial ends

Reference Sommerfeld number S and Sommerfeld number for the inner and outer films, S_1 and S_2 are defined as follows:

$$S = \frac{\eta R_1^3 L\omega_j}{\pi W_j C_1^2} \quad (3a)$$

$$S_1 = \frac{\eta R_1^3 L(\omega_j+\omega_r)}{\pi W_j C_1^2} = (1+\alpha)S \quad (3b)$$

$$S_2 = \frac{\eta R_2^3 L(\omega_r+\omega_b)}{\pi (W_j+W_r) C_2^2} = \frac{(\alpha+\gamma)\delta^3 S}{(1+\sigma)\beta^2} \quad (3c)$$

where

α : dimensionless ring speed $= \omega_r/\omega_j$

β : clearance ratio $= C_2/C_1$

γ : dimensionless sleeve speed $= \omega_b/\omega_j$

δ : diameter ratio $= D_2/D_1$

σ : weight ratio $= W_r/W_j$

From equations (1a) and (1b), the following equation for force balance is obtained in nondimensional form.

$$G_1(\alpha,\varepsilon_2) = S_2 - \frac{(\alpha+\gamma)\delta^3 S_1}{\beta^2(1+\alpha)(1+\sigma)} = 0 \quad (4)$$

Friction factors at the inner and outer surfaces of the ring are obtained ad follows:

$$\left(\frac{R}{C}f\right)_{b1} = \frac{T_{b1}}{W_j C_1} = -\frac{1}{2}\varepsilon_1\sin(\phi_1)+\frac{1-\alpha}{1+\alpha}\pi S_1 I_1 \quad (5a)$$

$$\left(\frac{R}{C}f\right)_{j2} = \frac{T_{j2}}{(W_j+W_r)C_2} = \frac{1}{2}\varepsilon_2\sin(\phi_2)+\frac{\alpha-\gamma}{\alpha+\gamma}\pi S_2 I_2 \quad (5b)$$

where

$$I_1 = \iint_{\Omega_{f1}}\frac{1}{1+\varepsilon_1\cos\theta_1}d\theta_1 dZ + \iint_{\Omega_{c1}}\frac{1+\varepsilon_1\cos\theta_{c1}}{(1+\varepsilon_1\cos\theta_1)^2}d\theta_1 dZ$$

$$I_2 = \iint_{\Omega_{f2}}\frac{1}{1+\varepsilon_2\cos\theta_2}d\theta_2 dZ + \iint_{\Omega_{c2}}\frac{1+\varepsilon_2\cos\theta_{c2}}{(1+\varepsilon_2\cos\theta_2)^2}d\theta_2 dZ$$

θ_{c1}, θ_{c2} : angular coordinates of film rupture boundaries in the inner and outer films

Ω_{f1}, Ω_{f2} : full film regions in the inner and outer films

Ω_{c1}, Ω_{c2} : cavitation regions in the inner and outer films

Nondimensionalizing the equation (1c), the following equation for moment balance is obtained.

$$G_2(\alpha,\varepsilon_2) = \left(\frac{R}{C}f\right)_{b1} - \beta(1+\sigma)\left(\frac{R}{C}f\right)_{j2} = 0 \quad (6)$$

For the given L/D_1, L/D_2, β, γ, σ and ε_1, simultaneous equations (4) and (6) can be solved by the following Newton-Raphson method combined with underrelaxation. Iteration procedure was terminated if $|\Delta\alpha/\alpha|_k < 10^{-4}$ and $|\Delta\varepsilon/\varepsilon|_k < 10^{-4}$.

$$(\alpha,\varepsilon_2)^T_{k+1} = (\alpha,\varepsilon_2)^T_k - \kappa J_k^{-1}(G_1,G_2)^T_k \quad (7)$$

where

$$J_k = \begin{bmatrix}\frac{\partial G_1}{\partial\alpha} & \frac{\partial G_1}{\partial\varepsilon_2}\\ \frac{\partial G_2}{\partial\alpha} & \frac{\partial G_2}{\partial\varepsilon_2}\end{bmatrix}_k$$

Once α and ε_2 have been obtained, various steady state performances of the inner and outer films can be calculated.

3. Results and Discussion

There are several parameters affecting the performances of the floating ring journal bearing, such as slenderness ratios of the

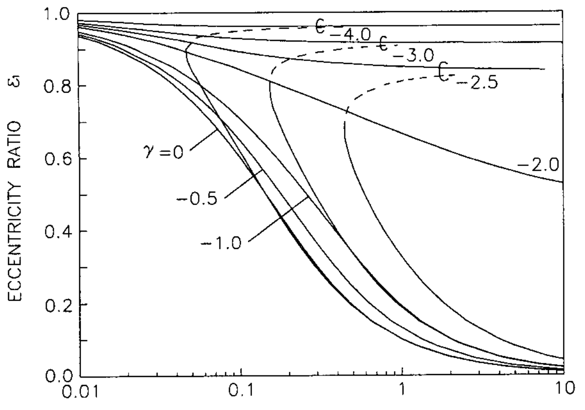

Fig. 2. Eccentricity ratio of inner film versus reference Sommerfeld number (—: stable state, ---- : unstable state).

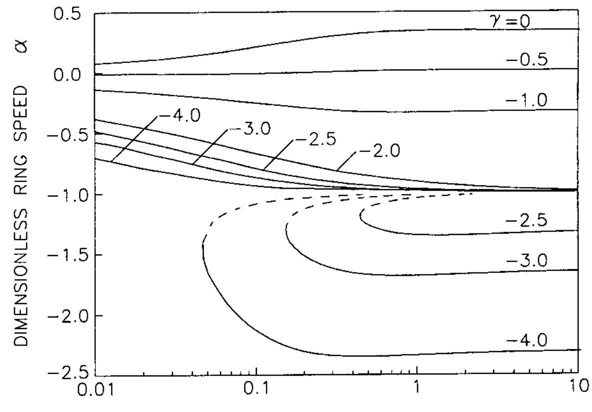

FIg. 4. Dimensionless ring speed versus reference Sommerfeld number (—: stable state, ---- : unstable state).

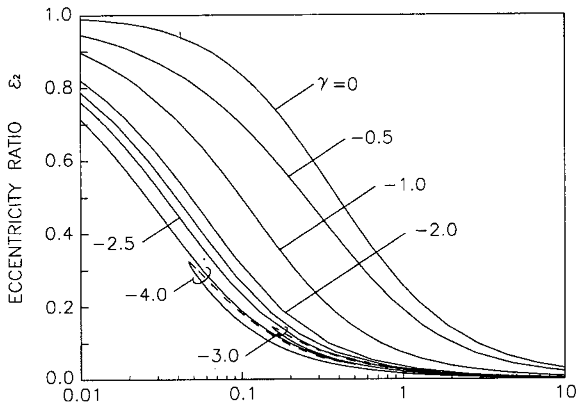

FIg. 3. Eccentricity ratio of outer film versus reference Sommerfeld number (—: stable state, ---- : unstable state).

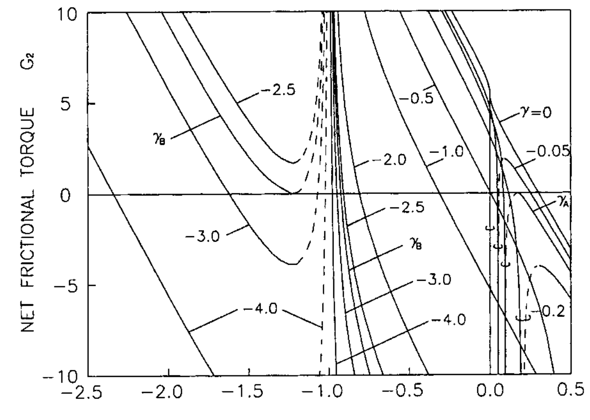

FIg. 5. Net frictional torque versus ring speed (—: stable state, ---- : unstable state).

inner and outer films, L/D_1 and L/D_2, weight ratio σ, diameter ratio δ, clearance ratio β and dimensionless counterrotating speed of the sleeve γ. In this paper the results are presented under the conditions that $L/D_1 = 1.0$, $L/D_2 = 0.8$, $\sigma = 0$ (i.e. the weight of the ring is neglected) and $\beta = 1.0$.

Fig. 2 and 3 show the eccentricity ratios of the inner and outer films as a function of reference Sommerfeld number. It can be seen that the floating ring journal bearing with the journal and sleeve counterrotating at equal speed ($\gamma = -1$) have considerable load capacity, while conventional journal bearing with one fluid film cannot. As the counterrotating speed of the sleeve increases, the eccentricity ratio of the inner film increases until the counterrotating speed of the sleeve reaches a certain critical value, and thereafter it continue to decrease, while the eccentricity ratio of the outer film continues to decrease from the beginning. Since the load capacity of the journal bearing is proportional to the absolute value of the sum of the velocities of the two interfacing surfaces, load capacity of the inner and outer films depend on $|\omega_j + \omega_r|$ and $|\omega_r + \omega_b|$, respectively.

As can be seen from Fig. 4 showing the variations of the ring speed with reference Sommerfeld number, if the counterrotating speed of the sleeve increases from zero, the ring rotating in the same direction with the journal in early stage is decelerated to be stationary, and then accelerated to the rotational direction of the sleeve. Hence, as the counterrotating speed of the sleeve increases, load capacity of the inner film decreases until $\omega_r = -\omega_r$ (i.e. $\alpha = -1$), and thereafter continues to increase, while load capacity of the outer film continues to increase from the beginning.

Fig. 2 shows that the curves have discontinuities due to the fact that, as the dimensionless ring speed approaches −1, load capacity of the inner film decreases and the reference Sommerfeld number increases drastically and diverges to infinity. Under these circumstances, the eccentricity of the outer film converges to zero so that the load capacity of the outer film can keep the balance with that of the inner film.

Fig. 2 to 4 are obtained under the condition of constant dimensionless sleeve speed, but in real operation, there can be several modes of raising the speeds of the journal and sleeve to the target speeds. Fig. 2 to 4 show that there can exist three equilibrium states for a reference Sommerfeld number, but true equilibrium state according to the operating modes cannot be seen from Fig. 2 to 4. Hence, the problem remained is to discriminate true equilibrium state, and if it is resolved, the operating characteristics of the counterrotating floating ring journal bearing is clarified.

Now, the operating mode that after the journal speed is raised to the target speed the sleeve is increased gradually from zero is considered and the operating condition of $S = 0.3$ is taken as a specific example. Increasing the counterrotating speed of the sleeve, the synchronous counterrotation in the inner film follows. If these circumstances are passed through, it is possible to raise the sleeve speed infinitely. The process of passing through the circumstances of the synchronous counterrotation in the inner and outer films can be explained by Fig. 5 which shows the relationship between the net frictional torque on the ring, defined in the equation (6), and the ring speed. Fig. 5 is obtained by determining equilibrium states of the inner and outer films for a given ring speed. Hence, the intersecting points between the curves of the net frictional torque and the line $G_2 = 0$ are the equilibrium states, and connecting the equilibrium states in the direction of γ decreasing, the behavior of the equilibrium states can be known. The stability of the equilibrium state can be discriminated from Fig. 5. At the equilibrium state with positive slope of the curve, if the ring speed increases somewhat by the external disturbance, G_2 becomes positive and the frictional torque exerted on the inner surface of the ring is larger than the frictional torque exerted on the outer surface of the ring. Therefore, α increases more and more, and the system cannot return to the original state. If α decreases somewhat by the external disturbance, α continues to decrease and the system cannot return to the original state. Hence, the equilibrium state with positive slope of the curve is unstable. At the equilibrium state with negative slope, although α varies somewhat by the external disturbance, restoring torque always makes the system maintain its original equilibrium state. Hence, the equilibrium state with negative slope is stable.

Increasing the counterrotating speed of the sleeve gradually. the synchronous counterrotation in the inner film occurs first. As can be shown from Fig. 5, decreasing γ from $\gamma = 0$, the stable state is experienced until γ becomes γ_A, and the system moves to the adjacent stable equilibrium state by jump phenomenon. Hence, the synchronous counterrotation in the outer film can always be passed through by small jump. If the counterrotating speed of the sleeve decreases further, the system continues to be in the stable equilibrium state, until the synchronous counterrotation in the inner film occurs. If α is very close to -1, the frictional torque exerted on the inner surface of the ring by the inner film can grow infinitely in theory. Accordingly, the ring speed cannot be less than $-\omega_j$ as far as quasistatic operation is carried out, which means that in Fig.5 there exist infinite number of lines and stable equilibrium states corresponding to γ less than -1 between the line $\alpha = -1$ and the declining curve corresponding to $\gamma = -4$, and likewise there exist infinite number of unstable equilibrium states between the line $\alpha = -1$ and the ascending curve corresponding to $\gamma = -4$. As γ decreases more, the gap between the two equilibrium states corresponding to a certain to γ becomes smaller. When α gets very close to -1, the system in

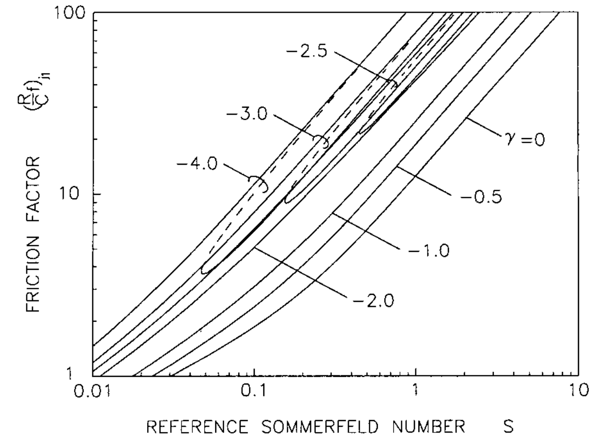

FIg. 6. Friction factor at journal versus reference Sommerfeld number (—: stable state, ---- : unstable state).

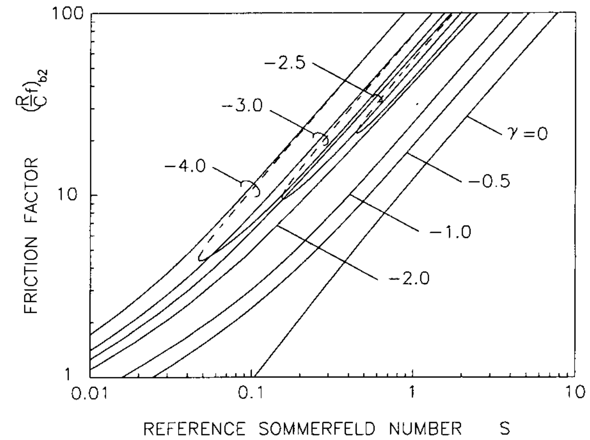

FIg. 7. Friction factor at sleeve versus reference Sommerfeld number (—: stable state, ---- : unstable state).

the stable state is liable to move to the adjacent unstable state by the external disturbance. Then the system cannot return to the original state any more and finally moves to the stable state where α is much smaller than -1 by jump phenomenon. Therefore, for considerably low γ, the stable equilibrium state in the neighborhood of the line $\alpha = -1$ is proven to be a kind of the unstable state. After passing through the synchronous counterrotation in the inner film, the system always experiences the stable equilibrium state as the counterrotating speed of the sleeve continues to increase.

Now, the process of decelerating the counterrotating speed of the sleeve is dealt with. In early stage, the stable equilibrium state is maintained, but when γ becomes γ_B, the equilibrium state of the system becomes unstable and the system moves to the stable state in the neighborhood of the line $\alpha = -1$. Thereafter the stable state is maintained until the system experiences another jump phenomenon at $\gamma = \gamma_A$. In this way, the counterrotating speed of the sleeve can be reduced to zero.

The operating mode that after the sleeve is raised to the target speed the journal speed is increased gradually can also be considered. In this case, the synchronous counterrotation in the inner film occurs first, and that in the outer film follows.

The synchronous counterrotation in the inner film can be passed through in the same way as that in the outer film of the former operating mode, while the synchronous counterrotation in the outer film can be passed through in the same way as that in the inner film of the former operating mode.

Fig. 4 also shows that in the case of at $\gamma=-0.5$, the ring speed is close to zero in broad range of reference Sommerfeld number. This means that the load capacities of the inner and outer films mainly owe to the rotation of the journal (at inner film) and sleeve (at outer film), respectively. Therefore, for a given counterrotating speed of the sleeve, it is possible to make the ring stationary if the clearance ratio is well chosen.

Fig. 6 and 7 show the friction factors at the journal and sleeve as a function of Sommerfeld number. Friction factors at both surfaces increase with γ decreasing. There is drastic change of the friction factors in the case of at $\gamma=-2.5$, -3.0 and -4.0, which results from the drastic change of the load capacities of the inner and outer films due to the synchronous counterrotation.

Conclusions

The steady state performance of the counterrotating floating ring journal bearings is analyzed with isothermal finite bearing theory. It is shown that counterrotating floating ring journal bearings properly designed have considerable load capacity at equal counterrotating speeds. Investigating the relationship between the net friction torque exerted on the ring by the inner and outer films and the rotational speed of the ring, it is shown that the synchronous counterrotation in the inner and outer film can be passed through by the jump phenomenon from the unstable equilibrium state to the stable state. The operating characteristics of the counterrotating floating ring journal bearing according to the method of acceleration and deceleration of the rotational speeds of the journal and sleeve are clarified. It is theoretically confirmed that floating ring journal bearings can be used in counterrotating journal-bearing system and have the potential to become good substitutes for rolling bearings in counterrotating systems.

Nomenclature

C	= clearance
D_1, D_2	= inner and outer diameters of ring
G_2	$=\left(\frac{R}{C}f\right)_{b1}-\beta(1+\sigma)\left(\frac{R}{C}f\right)_{j2}$, net friction torque on ring
f_p	= pressure force
h	$= C(1+\varepsilon\cos\theta)$, film thickness
J	= Jacobian matrix
L	= length of bearing and ring
R_1, R_2	= inner and outer radii of ring
$\left(\frac{R}{C}f\right)_{b1}$	$=\frac{T_{b1}}{W_jC_1}$, friction factor at inner surface of ring
$\left(\frac{R}{C}f\right)_{b2}$	$=\frac{T_{b2}}{W_jC_1}$, friction factor at sleeve
$\left(\frac{R}{C}f\right)_{j1}$	$=\frac{T_{j1}}{W_jC_1}$, friction factor at journal
$\left(\frac{R}{C}f\right)_{j2}$	$=\frac{T_{j2}}{(W_j+W_r)C_2}$, friction factor at outer surface of ring
S	$=\frac{\eta R_1^3L\omega_j}{\pi W_jC_1^2}$, reference Sommerfeld number
S_1	$=\frac{\eta R_1^3L(\omega_j+\omega_r)}{\pi W_jC_1^2}$, reference Sommerfeld number
S_2	$=\frac{\eta R_2^3L(\omega_r+\omega_b)}{\pi(W_j+W_r)C_2^2}$, reference Sommerfeld number
T	= torque exerted on ring
u	= linear velocity of surface
W_j, W_r	= load on bearing and weight of ring
z, Z	= axial coordinate and dimensionless axial coordinate
α	$=\omega_r/\omega_j$, dimensionless ring speed
β	$=C_2/C_1$, clearance ratio
γ	$=\omega_b/\omega_j$, dimensionless bearing speed
ε	= eccentricity
η	= absolute viscosity of lubricant
θ	= angle measured from position of maximum film thickness
κ	= underrelaxation factor
ρ	= density of lubricant
σ	$=W_r/W_j$, weight ratio
ω_j, ω_r, ω_b	= angular velocities of journal, ring, bearing

Superscripts and Subscripts

-1	refer to inverse
1	refer to inner film
2	refer to outer film
b, j	refer to the surfaces corresponding to bearing and journal in the flm
k	refer to k-th iteration
x	refer to load direction
T	refer to transpose

References

1. Vance, J.M., Rotordynamics of Turbomachinery, John Wiley & Sons, Inc., pp. 45-47, 1988.
2. Pinkus, O., Counterrotating Journal Bearing, ASME Journal of Basic Engineering, Vol. 84, pp.110-115, 1962
3. Orcutt, F. K. and Ng, C. W., Steady-State and Dynamic Properties of the Floating-Ring Journal Bearing, ASME Journal of Lubrication Technology, Vol. 90, pp. 243-253, 1968.

4. Tanaka, M. and Hori, Y., Stability Characteristics of Floating Bush Bearings, ASME Journal of lubrication Technology, Vol. 94, pp. 248-259, 1972.
5. Li, C. H. and Rohde, S. M., On the Steady State and Dynamic Performance Characteristics of Floating Ring Bearings, ASME Journal of Lubrication Technology, Vol. 103, pp. 389-397, 1981.
6. Wilcock, D. F., Load Carrying Efficiency of Floating Ring Journal Bearings, ASME Journal of Lubrication Technology, Vol. 105, pp. 605-608, 1983.